Characteristics of a micro dielectric barrier discharge ignited by a cold cathode with high ion-induced secondary electron emission for plasma display panel

Giichiro Uchida,[1,a] Satoshi Uchida,[2] Hiroshi Kajiyama,[1] and Tsutae Shinoda[1]
[1]*Graduate School of Advanced Science of Matter, Hiroshima University, Higashi-Hiroshima 739-8530, Japan*
[2]*Graduate School of Science and Engineering, Tokyo Metropolitan University, Hachioji 192-0397, Japan*

(Received 3 September 2009; accepted 23 September 2009; published online 2 November 2009)

We present here measurements of plasma display panel (PDP) ignited by SrO and SrCaO cold cathodes with high yield of ion-induced secondary electron emission (high γ_i). SrO- and SrCaO-cathode PDPs attain high luminous efficacy at low applied voltage, where the breakdown voltage is 30% lower than that of ordinary MgO-cathode PDP. Current and emission measurement clearly demonstrates that SrO- and SrCaO-cathode PDPs operated at low voltage realize a discharge with smaller current flow and lower electron energy, which are considerably appropriate for high luminous efficacy of PDP. Simulation analysis shows the effect of the high-γ_i cathode on the luminous efficacy of PDP. A discharge ignited by the high-γ_i cathode realizes high electron heating efficiency due to the abundant seed electrons from the high-γ_i cathode, resulting in high luminous efficacy of PDP. © *2009 American Institute of Physics*. [doi:10.1063/1.3253723]

I. INTRODUCTION

Plasma display panel (PDP) utilizing the vacuum ultraviolet (VUV) emission from micro dielectric barrier discharge (micro-DBD) is the present interesting topic in atmospheric microplasma physics and engineering.[1,2] The fundamental property of microdischarge in a PDP cell has been experimentally investigated for the last 10 years,[3–12] and the high Xe concentration of the discharge gas becomes one of the most promising approaches to improve the luminous efficiency.[13,14] But, the condition of high Xe partial pressure accompanies an increase in breakdown voltage, and the development of new cathode material is strongly required for low voltage PDP operation. One of our interests has been concerned with PDP ignited by a cold cathode with high secondary electron emission induced by the impinging ion, where the yield of secondary electron emission γ_i is defined as the number of electrons emitted from the cathode per an incident ion. It has been well known that high-γ_i material is advantageous for low breakdown voltage, and various chemically active materials such as SrO and SrCaO have been already applied to PDP.[15] Recently, Motoyama *et al.* and other groups have demonstrated high luminous efficacy in SrCaO-cathode color PDP at low sustaining voltage[16–19] and suggested the possibility of high Xe-pressure PDP as a commercial product in the future. However, the detailed feature of the SrCaO-cathode discharge is still not clear, and more basic experiment is required to control and optimize the high-γ_i cathode discharge for PDP. The main purpose of this study is to analyze the characteristics of the micro-DBD ignited by the high-γ_i cathode, and SrO and SrCaO are also applied to a cold cathode in our experiment. The measurement clearly demonstrates that SrO and SrCaO cathodes can ignite a discharge at a lower voltage, resulting in smaller current flow and lower electron energy. The plasma condition is considerably appropriate for PDP, and high luminous efficacy is attained in the low voltage operation of high-γ_i PDP. The effect of the high-γ_i cathode on the luminous efficacy is theoretically analyzed by using a one-dimensional fluid model. The high-γ_i cathode causes high electron heating efficiency due to the abundant seed electron, resulting in high luminous efficacy of PDP.

At first, we report experiments of SrO- and SrCaO-cathode PDPs. Then, we present the simulation analysis of PDP with the high-γ_i cathode.

II. EXPERIMENTS

A panel characteristic such as the luminous efficacy is measured in the experimental room filled with Ne/Xe gas mixture without panel sealing. The electrode of the front panel is a standard stripe with 180 μm in width, and the interelectrode distance between the X and Y electrodes is 80 μm, as shown in Fig. 1(a). The display area is 12 $\times$ 48 mm^2 (170 $\times$ 18 cells), and the electrodes are covered by the dielectric layer of 30 μm and then a 500 nm thick protective layer. Three color phosphors of red ($(Y,Gd,Eu)BO_3$), green ($Zn_2SiO_4:Mn$), and blue [$(Ba,Eu)MgAl_{10}O_{17}$] are deposited on the rear panel, and colored PDPs are evaluated in experiment. The PDP discharge is operated by applying the 15 kHz square sustaining voltage (V_s=90–300 V) to the pair sustaining electrodes. Values of a first-cell breakdown voltage (V_{f1}) are listed in Table I. The breakdown voltage (V_{f1}) of SrO and SrCaO panels is as low as about 70% with respect to that of the ordinary MgO-cathode panel. This result clearly demonstrates that SrO and SrCaO have higher γ_i compared with that of MgO and is considerably effective for decreasing the breakdown voltage of PDP.

Figures 2(a) and 2(b) show the luminance (L) and the luminous efficacy (η) of SrO- and MgO-colored (red, green, and blue) panels as a function of the sustaining voltage (V_s),

[a]Electronic mail: giichiro@hiroshima-u.ac.jp.

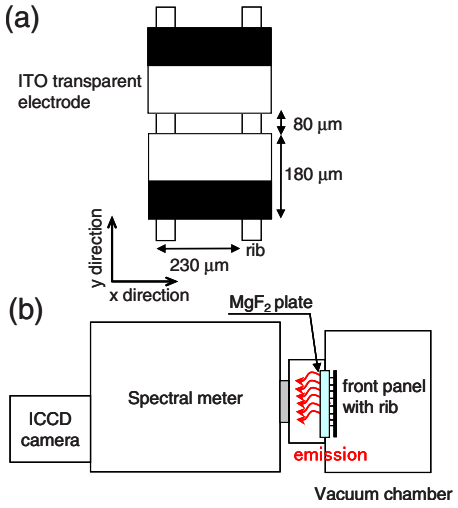

FIG. 1. (Color online) (a) A cell structure and (b) schematic of experimental setup for emission measurement.

where a breakdown voltage (V_{f1}) of each panel is marked by arrows. The L drastically increases with V_s especially for high Xe concentration (C_{Xe}) of 20%, as shown in Fig. 2(a). For low Xe concentration of 4%, η increases abruptly below 150 V corresponding to the static margin of the SrO panel, and the SrO panel achieves 1.5 times η with respect to the ordinary MgO panel, as found in Fig. 2(b). Also for C_{Xe} =20%, η of the SrO panel drastically increases as V_s decreases, and high η of 2.5 lm/W is attained at low V_s of 130 V. We can also find interesting fact that comparing SrO and MgO panels at the same applied voltage, for example, V_s =180 and 190 V for C_{Xe}=20% in Fig. 2(b), the SrO panel shows higher η than that of the ordinal MgO panel. The result clearly indicates that the γ_i value has influence not only on the breakdown voltage but also on the luminous efficacy of PDP. The effect of high γ_i on η is theoretically discussed by using simulation method in Sec. III.

Then, emission measurement[4,13,20] is performed using a specified panel in order to analyze the characteristic of high performance SrO- and SrCaO-cathode PDPs, where barrier ribs are manufactured on the front panel and the MgF_2 glass is applied as a real panel, as schematically shown in Fig. 1(b). The dimension of the cell is completely the same as the panel used in L and η measurements. Figure 3 shows the spatiotemporal profile of infrared (IR) emission from the Xe excited atom. The results are presented for (a) SrCaO-PDP and (b) MgO-PDP at various applied voltages under the condition of Ne/Xe (20%) gas pressure=67 kPa. At the breakdown voltage of 190 V of SrCaO-PDP, the IR emission appears around the center of the cathode and anode electrodes (y=220 μm) and moves toward the periphery of the cathode electrode at a velocity of 2.0×10^3 m/s. As V_s is increased to 240 V, IR emission rapidly spreads over the whole electrodes, and the discharge time becomes as short as approximately 50 ns. The right pictures also show the spatial profile of IR emission at 200 and 170 ns when an emission peak is observed for V_s=190 and 240 V, respectively. At low V_s of 190 V, only weak emission is observed above the cathode area, while at V_s=240 V (high voltage), strong IR emission covers both over the cathode and anode areas. For MgO-PDP, on the other hand, IR emission suddenly spreads and covers over whole electrodes both at 240 and 270 V, where 270 V corresponds to the breakdown voltage of MgO-PDP.

TABLE I. Comparison of a first-cell breakdown voltage (V_{f1}) of SrO-, SrCaO-, and MgO-cathode PDPs.

Gas condition	Protective layer	V_{f1} (V)
Ne/Xe (4%) 67 kPa	MgO	204
Ne/Xe (4%) 67 kPa	SrO	144
Ne/Xe (4%) 67 kPa	SrCaO	148
Ne/Xe (20%) 67 kPa	MgO	269
Ne/Xe (20%) 67 kPa	SrO	191
Ne/Xe (20%) 67 kPa	SrCaO	196

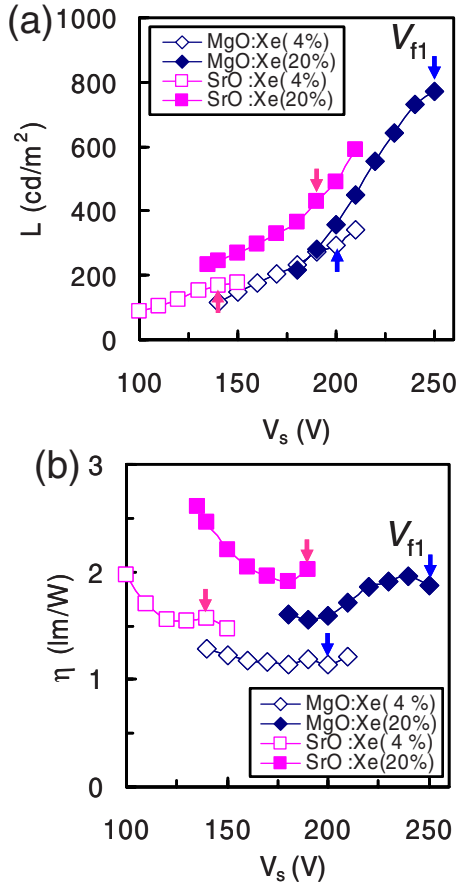

FIG. 2. (Color online) Sustaining voltage (V_s) dependence of (a) luminance (L) and (b) luminous efficacy (η) for Xe concentrations (C_{Xe}) of 4% and 20% at a Ne/Xe gas pressure of 67 kPa. A breakdown voltage (V_{f1}) of each panel is marked by arrows.

In Fig. 4(a), discharge current pulses are plotted as a function of V_s. Extremely small discharge current is observed to flow in the low voltage operation of 190 V of SrCaO-cathode PDP. Increasing V_s leads to a larger current peak, accompanied with the shortening of discharge formation time lag. The current peak value (I_{peak}) is also found to increase linearly to V_s, as shown in Fig. 4(b), where a breakdown voltage (V_{f1}) of each panel is marked by arrows. From these experiments, it is shown clearly that the lower V_s operation of SrCaO-PDP realizes a weak discharge with small current flow.

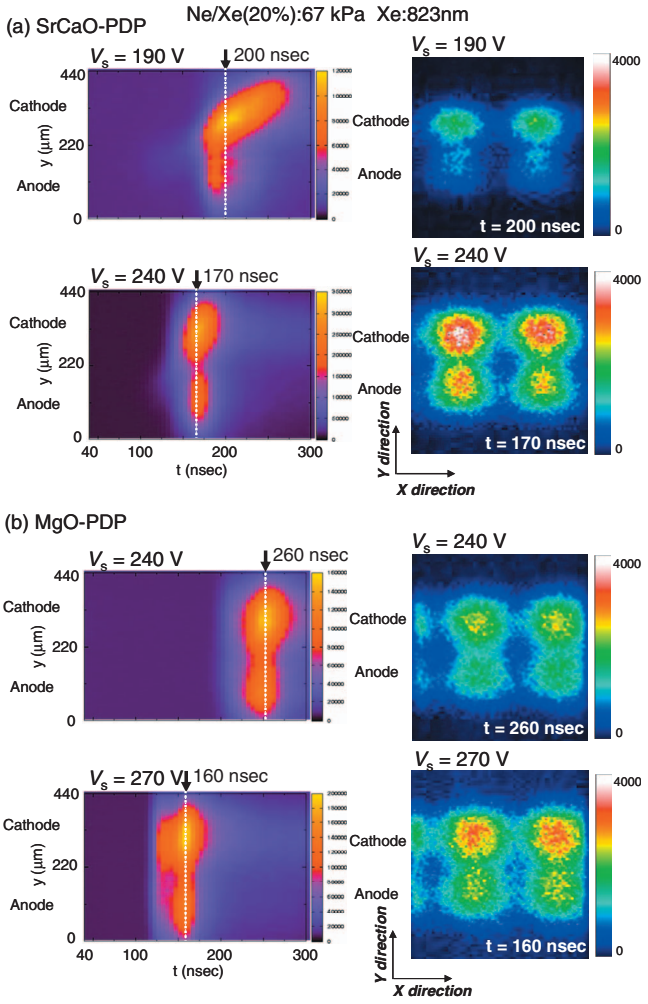

FIG. 3. (Color) Spatiotemporal behaviors of IR emission from the Xe excited atom with 823 nm in wavelength at various sustaining voltages (V_s). Ne/Xe (20%) gas pressure=67 kPa. (a) and (b) are SrCaO- and MgO-cathode PDPs, respectively.

Then, the emission ratio from Ne and Xe atoms ($I_{\mathrm{Ne(585\ nm)}}/I_{\mathrm{Xe(823\ nm)}}$) is analyzed in order to evaluate the electron energy in micro-DBD in a PDP small cell. The precursor state of 585 nm emission from the Ne atom is 18.96 eV, while that of 823 nm emission from the Xe atom is only 9.82 eV. Therefore, Ne emission is an indication of the existence of relatively high energy electron, and the variety of electron energy can be roughly estimated by observing the intensity of Ne emission relative to Xe emission. Figure 5 gives the temporal evolution of $I_{\mathrm{Ne(585\ nm)}}/I_{\mathrm{Xe(823\ nm)}}$ for (a) MgO- and (b) SrO-cathode panels as a parameter of V_s at Ne/Xe (4%) pressure of 67 kPa. Arrows in the figure denote a time when a peak of the Ne emission ($I_{\mathrm{Ne(585\ nm)}}$) is observed. The fraction of the Ne emission is extremely high in the initial stage of the discharge and drastically decreases with time. The result clearly demonstrates the transient behavior of electron energy (E_e) that E_e is quite high in the early stage and exhibits a decrease with time.[21] The V_s is also changed to study the effect of the space electric field on the electron energy in detail. Figures 6(a) and 6(b) are $I_{\mathrm{Ne(585\ nm)}}/I_{\mathrm{Xe(823\ nm)}}$ for C_{Xe}=4% and 20%, respectively, and the emission intensity is averaged over half cycle of the

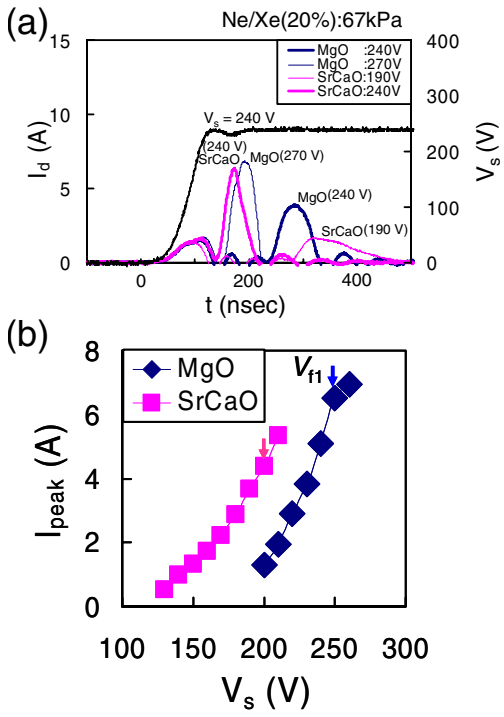

FIG. 4. (Color online) (a) Discharge current pulses of SrCaO- and MgO-cathode PDPs and (b) sustaining voltage (V_s) dependence of a peak current value (I_{peak}).

sustain phase. Here, a breakdown voltage (V_{f1}) of each panel is marked by arrows. The $I_{\mathrm{Ne(585\ nm)}}/I_{\mathrm{Xe(823\ nm)}}$, which corresponds to electron energy, increases linearly with V_s both for C_{Xe}=4% and 20%. This clearly indicates that lower V_s operation of SrO-PDP can realize the lower electron energy in micro-DBD. Based on the panel measurements, we can conclude that SrO and SrCaO cathodes can ignite a discharge at a low voltage, resulting in smaller current flow and lower

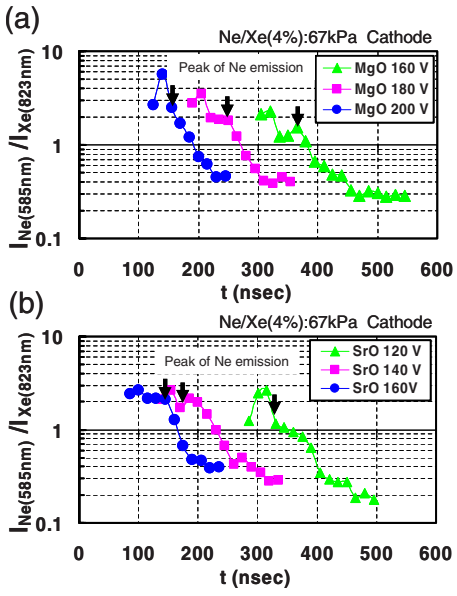

FIG. 5. (Color online) Temporal evolution of relative spectrum intensity of Ne ($I_{\mathrm{Ne(585\ nm)}}$) and Xe ($I_{\mathrm{Xe(823\ nm)}}$) emissions as a parameter of sustaining voltage (V_s). (a) and (b) are MgO- and SrO-cathode PDPs, respectively. Ne/Xe (4%) gas pressure is 67 kPa, and arrows show the time when the Ne-emission peak is observed.

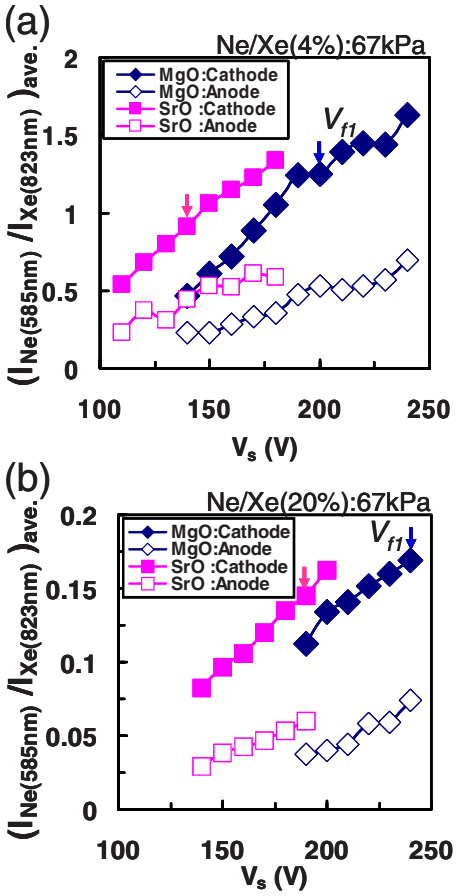

FIG. 6. (Color online) The sustaining voltage (V_s) dependence of relative spectrum intensity of Ne ($I_{Ne(585\ nm)}$) and Xe ($I_{Xe(823\ nm)}$) emissions. (a) and (b) are Xe concentrations of 4% and 20%, respectively. The emission intensity is averaged over half cycle of the sustain phase, and a breakdown voltage (V_{f1}) of each panel is marked by arrows.

electron energy. The plasma conditions are considerably appropriate for PDP, and high luminous efficacy is attained in lower voltage operation of SrO-cathode PDP, as shown in Fig. 2(b).

III. SIMULATION ANALYSIS

We perform simulation analysis on a micro-DBD[22–25] ignited by the high-γ_i cold cathode using a one-dimensional fluid model in order to promote our basic knowledge of discharge characteristics in the high-γ_i cathode PDP. A focus is on the effect of high γ_i induced by the impinging Xe ion (γ_{Xe}) on a micro-DBD because the γ_{Xe} is more important than the neon-ion-induced γ_i for PDP with high Xe contents. In our calculation, the yield of secondary electron emission induced by Ne ion (γ_{Ne}) and the sustaining voltage (V_s) are fixed at 0.35 and 400 V, respectively. Here, the reaction processes in this simulation are listed in Ref. 26. Figure 7 shows discharge current pulses as a parameter of γ_{Xe}. It is clearly observed that increasing γ_{Xe} leads to a larger current peak, which accompanies the shortening of discharge formation time lag and current rise time. Also, in our experiment, SrCaO-PDP with the high-γ cathode has a larger current peak compared with that of ordinal MgO-PDP at V_s =240 V, as shown in Fig. 4(a), which is well consistent with the calculation result. Then, the spatial profiles of plasma

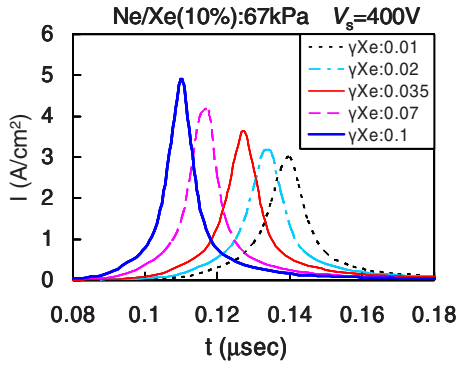

FIG. 7. (Color online) Discharge current pulses as a parameter of secondary electron emission yield induced by the impinging Xe ion to the cathode (γ_{Xe}). Here, the yield of secondary electron emission induced by the Ne ion (γ_{Ne}) is fixed at 0.35. The sustaining voltage (V_s) is 400 V.

parameters are compared between discharges ignited by the cathode with γ_{Xe}=0.035 and 0.1. Figures 8(a)–8(c) show space potential (V_p) and electric field intensity (E), electron temperature (T_e), and electron and ion densities (n_e and n_i), respectively, as a function of the distance from the cathode position. Here, space profiles of the plasma parameter are plotted at the current peak time, and the cathode and anode electrodes are set at 0 and 80 μm, respectively. As can be seen in Fig. 8(a), the typical ion-sheath structure with strong electric field is observed in front of the cathode electrode. The electron temperature is quite high in the sheath region due to the acceleration of electrons by the sheath electric field and drastically decreases with distance from the cathode, as shown in Fig. 8(b). Ions concentrate in the ion-sheath region, and the plasma region, which consists of the same number of electrons and ions, is observed at 20 μm far from

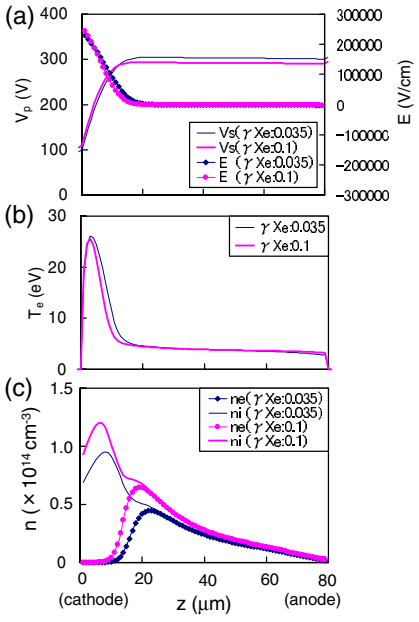

FIG. 8. (Color online) Comparison of plasma parameters between discharges ignited by the cathode with γ_{Xe}=0.035 and 0.1. Here, the yield of secondary electron emission induced by the Ne ion (γ_{Ne}) is fixed at 0.35. (a), (b), and (c) show spatial profiles of space potential (V_p) and electric field intensity (E), electron temperature (T_e), and electron and ion densities (n_e and n_i), respectively. The plasma parameters are plotted at the current peak time. The sustaining voltage (V_s) is 400 V.

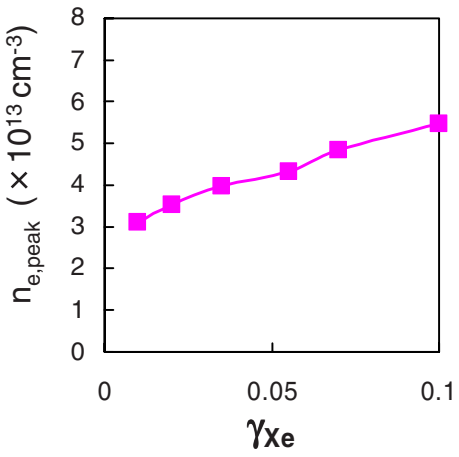

FIG. 9. (Color online) Dependence of electron density (n_e) as a function of the Xe-ion-induced γ_i, where a peak of electron density ($n_{e,peak}$) is plotted. The yield of secondary electron emission induced by the Ne ion (γ_{Ne}) is fixed at 0.35. The sustaining voltage (V_s) is 400 V.

the cathode [see Fig. 8(c)]. It should be noted that the drastic increase in the charged particle of ion and electron is found by increasing γ_{Xe} from 0.035 to 0.1, as found in Fig. 8(c), although no significant change is seen in the space potential and the electron energy in Figs. 8(a) and 8(b). Figure 9 summarizes the γ_{Xe} dependence of electron density, where a peak value of electron density ($n_{e,peak}$) is plotted. The $n_{e,peak}$ behaves linear to γ_{Xe}, and high density plasma is realized at high γ_{Xe}. In our experiment, the stronger emission and larger current peak are observed from SrCaO-PDP rather than MgO-PDP when two panels are compared at the same operation voltage of 240 V, as shown in Figs. 3 and 4(a), respectively. The strong emission and large current of SrCaO-PDP are well explained by calculation result that the high-γ_i cathode leads to a drastic increase in plasma density.

In Fig. 10, the VUV radiation efficiency (η_{vuv}) is plotted as a function of γ_{Xe} at gas pressure=67 and 93 kPa. Here, η_{vuv}, which corresponds to the luminous efficacy (η) in the experiment, is defined as the ratio of the total VUV radiation energy relative to the electrical input energy. In the same manner as $n_{e,peak}$, the η_{vuv} increases linearly to γ_{Xe}.[24] It must

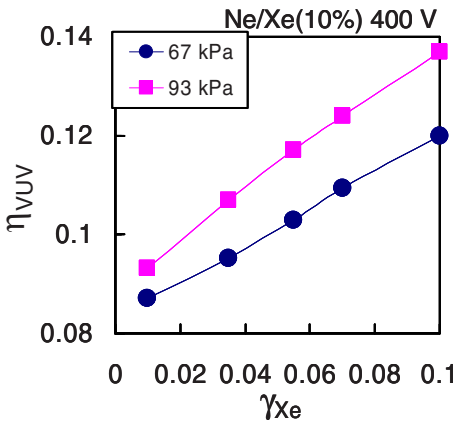

FIG. 10. (Color online) Dependence of the VUV radiation efficiency (η_{vuv}) as a function of secondary electron emission yield induced by the Xe ion (γ_{Xe}) at Ne/Xe pressure=67 and 93 kPa. Here, the yield of secondary electron emission induced by the Ne ion (γ_{Ne}) is fixed at 0.35. The sustaining voltage (V_s) is 400 V.

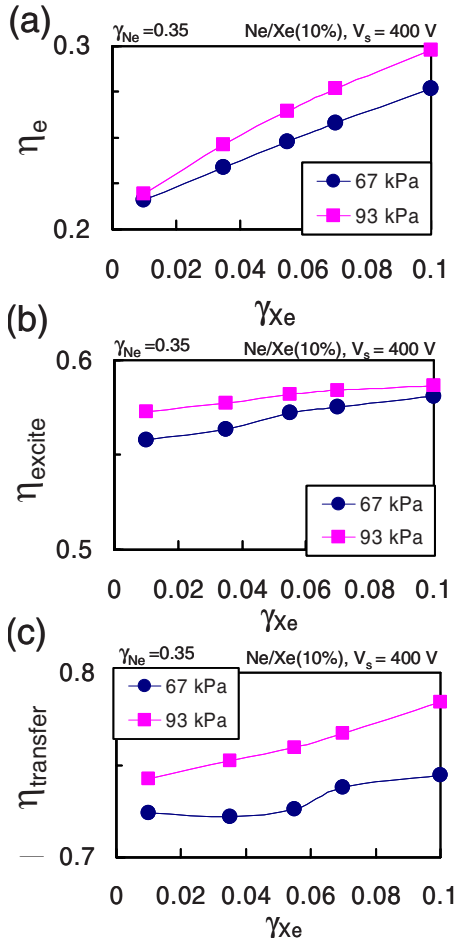

FIG. 11. (Color online) The Xe-ion-induced γ_i dependence of (a) electron heating efficiency (η_e), (b) Xe excitation efficiency (η_{excite}), and (c) efficiency of energy transferred from the excited Xe atom to the vuv radiation ($\eta_{transfer}$). Here, the yield of secondary electron emission induced by the Ne ion (γ_{Ne}) is fixed at 0.35. The sustaining voltage (V_s) is 400 V.

be emphasized that the increase of VUV efficiency at high γ_i is clearly observed also in our experiment. As shown in Fig. 2(b) obtained in our experiment, SrO-cathode PDP with high γ_i attains high luminous efficacy compared with that of the ordinal MgO-PDP at 180 and 190 V for C_{Xe}=20%, which well agrees with the calculation result. The calculated η_{vuv} is also divided into three parts according to the energy flow in a PDP cell from the input electrical energy to the output vuv radiation energy, i.e., (a) electron heating efficiency (η_e), (b) Xe excitation efficiency (η_{excite}), and (c) efficiency transferred from the Xe excited atom to the VUV radiation ($\eta_{transfer}$).[3,9,10,24,25] η_e is defined as the ratio of energy to be transferred to electron from the electrical input energy, and $\eta_{excitation}$ is the efficiency related to the production of Xe excited atom via the collision with the electron and Xe neutral atom. $\eta_{transfer}$ also shows the ratio of energy converted to vuv radiation from the Xe excited atom. As seen in Fig. 11, η_e is observed to drastically increase with γ_{Xe}, and also η_{excite} and $\eta_{transfer}$ exhibit a slight increase. This result shows that the high-γ_i cathode considerably contributes to high η_e of PDP.

Finally, the dynamic behavior of η_e is analyzed with transient plasma parameters. Figure 12 shows the temporal

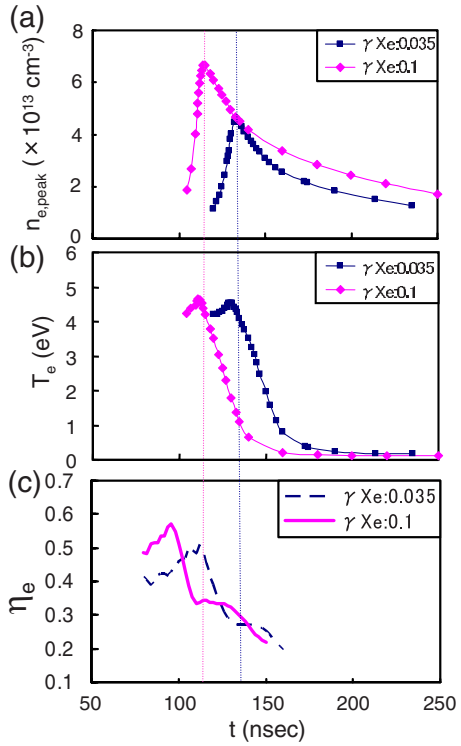

FIG. 12. (Color online) The temporal profiles of (a) electron peak density ($n_{e,peak}$), (b) electron temperature (T_e), and (c) electron heating efficiency (η_e) at γ_{Xe}=0.035 and 0.1. Here, the yield of secondary electron emission induced by the Ne ion (γ_{Ne}) is fixed at 0.35. The sustaining voltage (V_s) is 400 V.

profiles of (a) electron peak density ($n_{e,peak}$), (b) electron temperature (T_e), and (c) electron heating efficiency (η_e) at γ_{Xe}=0.035 and 0.1. As seen in Fig. 12(a), the rapid growth of discharge and consequent high plasma density are observed at high γ_{Xe} of 0.1, and these are major effects of the abundant seed electrons emitted from high-γ_i cathode. Also, high η_e is attained in the early stage of the pulse discharge with high γ_{Xe} value [see Fig. 12(c)], and these results clearly indicate that more frequent ionizations in the initial stage of discharge are quite effective for realizing high η_e. The shorter-pulse discharge characterized by the rapid growth of discharge is considered to be efficient in the electron heating[6,7] because in the later stage of pulse discharge, η_e becomes very low, as shown in Fig. 12(c), due to the significant dissipation of the input power to many ions concentrated in the cathode sheath, namely, the dominating ion heating loss in the ion sheath. Our calculation demonstrates that the high-γ_i cathode causes the rapid plasma production, which is quite efficient in the electron heating.

IV. CONCLUSION

We have described our measurement and simulation of PDP with the high-γ_i cathode. SrO- and SrCaO-cathode PDPs operated at low V_s realize small current flow and low electron energy, which are appropriate for high luminous efficacy of PDP. Simulation analysis theoretically shows the effect of the high-γ_i cathode on the luminous efficacy. The VUV radiation efficiency increases linearly to γ_{Xe} accompanied with a drastic increase in charged particle. The phenomena can be explained by the effect of abundant seed electrons from the high-γ_i cathode. The heated many seed electrons induces the rapid growth of discharge and consequent high plasma density, which are quite efficient in the electron heating due to less ion heating loss.

In conclusion, our study clearly demonstrates the advantage of high-γ_i PDP not only for low breakdown voltage but also for high luminous efficacy. Detailed feature of high-γ_i discharge would be quite important for realizing high performance PDP with high Xe concentration.

ACKNOWLEDGMENTS

This work was partly supported by the New Energy Development Organization (NEDO) and the Advanced PDP Development Center Corp. (APDC). We would like to thank ULVAC Inc. for the PDP experiment system. G.U. acknowledges stimulating discussions with T. Akiyama and also thanks N. Awaji and T. Yano for their technical support.

[1] T. Shinoda, M. Wakitani, T. Nanto, N. Awaji, and S. Kanagu, IEEE Trans. Electron Devices **47**, 77 (2000).
[2] J. P. Boeuf, J. Phys. D: Appl. Phys. **36**, R53 (2003).
[3] G. Oversluizen, K. Itoh, T. Shiga, and S. Mikoshiba, J. Appl. Phys. **104**, 033303 (2008).
[4] G. Oversluizen, M. Klein, S. de Zwart, S. van Heusden, and T. Dekker, Appl. Phys. Lett. **77**, 948 (2000).
[5] G. Oversluizen, M. Klein, S. de Zwart, S. van Heusden, and T. Dekker, J. Appl. Phys. **91**, 2403 (2002).
[6] G. Oversluizen and T. Dekker, J. Soc. Inf. Disp. **13**, 889 (2005).
[7] G. Oversluizen and T. Dekker, IEEE Trans. Plasma Sci. **34**, 305 (2006).
[8] M. F. Gillies and G. Oversluizen, J. Appl. Phys. **91**, 6315 (2002).
[9] W. J. Chung, B. J. Shin, T. J. Kim, H. S. Bae, J. H. Seo, and K. W. Whang, IEEE Trans. Plasma Sci. **31**, 1038 (2003).
[10] H. S. Bae, W. J. Chung, and K. W. Whang, J. Appl. Phys. **95**, 30 (2004).
[11] H. S. Bae, J. K. Kim, H. Y. Jung, J. K. Lim, and K. W. Whang, J. Appl. Phys. **102**, 123308 (2007).
[12] T. Akiyama, T. Yamada, M. Kitagawa, and T. Shinoda, J. Soc. Inf. Disp. **17**, 121 (2009).
[13] T. Yoshioka, L. Tessier, A. Okigawa, and K. Toki, J. Soc. Inf. Display **8**, 203 (2000).
[14] G. Oversluize, S. de Zwart, S. van Heusden, and T. Dekker, J. Soc. Inf. Disp. **8**, 197 (2000).
[15] T. Shinoda, H. Uchiike, and S. Andoh, IEEE Trans. Electron Devices **26**, 1163 (1979).
[16] Y. Motoyama and T. Kurauchi, J. Soc. Inf. Disp. **14**, 487 (2006).
[17] Y. Motoyama, Y. Murakami, M. Seki, T. Kurauchi, and N. Kikuchi, IEEE Trans. Electron Devices **54**, 1308 (2007).
[18] G. Uchida, K. Uchida, H. Kajiyama, and T. Shinoda, Proceedings of Society for Information Display 2008 International Symposium (SID '08), Los Angeles, CA, 2008, p. 1762.
[19] K. W. Whang, H. S. Bae, H. Y. Jung, and O. Kwon, Proceedings of the Eighth International Meeting on Information Display (IMID2008), Seoul, Korea, 2008, p. 153.
[20] K. Suzuki, Y. Kawanami, S. Ho, N. Uemura, Y. Yajima, N. Kouchi, and Y. Hatano, J. Appl. Phys. **88**, 5605 (2000).
[21] Y. Noguchi, A. Matsuoka, K. Uchino, and K. Muraoka, J. Appl. Phys. **91**, 613 (2002).
[22] J. Meunier, P. Belenguer, and J. P. Boeuf, J. Appl. Phys. **78**, 731 (1995).
[23] S. Rauf and M. J. Kushner, J. Appl. Phys. **85**, 3460 (1999).
[24] G. J. Hagelaar, M. H. Klein, R. M. M. Snijkers, and G. M. W. Kroesen, J. Appl. Phys. **89**, 2033 (2001).
[25] D. Hayashi, G. Heusler, G. Hagelaar, and G. Kroesen, J. Appl. Phys. **95**, 1656 (2004).
[26] T. Kubota, S. Uchida, and F. Tochikubo, Jpn. J. Appl. Phys. **48**, 046001 (2009).